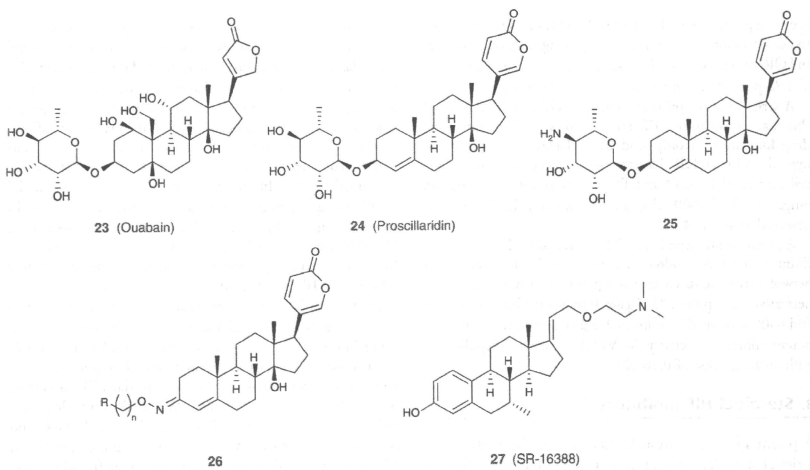

Figure 5. Steroidal HIF inhibitors.

SR-16388 was reduced to about 50% compared to the untreated control group. Furthermore, a combination of SR-16388 at 10 mg/kg and paclitaxel at 7.5 mg/kg produced a much greater inhibition of tumor growth over time. *In vitro* experiments showed that SR-16388 selectively binds to estrogen receptor β (ERβ) with high affinity. Recently, SRI International reported that SR-16388 binds selectively to estrogen-related receptor α (ERRα), but not to ERRβ or ERRγ, and inhibits transcriptional activity of ERRα [79]. However, the relationship between HIF inhibition and ERβ/ERRα inhibition by SR-16388 was not discussed.

4. Peptidic HIF inhibitors

The California Institute of Technology claimed DNA-binding polyamide [80]. The *N*-methylpyrrole and *N*-methylimidazole subunits in polyamide **28** (**Figure 6**) are able to bind to DNA comprising the sequence of 5′-WTWCGW-3′, wherein W is A or T, and the fluorophore (fluorescein isothiocyanate) in the tail of polyamide **28** is able to show its intracellular localization. The interaction of polyamide **28** and HRE (5′-TACGTG-3′) reduces the binding of HIF to HRE, thereby, inhibiting the expression of HIF-inducible genes that include VEGF, VEGF receptor-1 (Flt-1), endothelin-1, endothelin-2, endothelin-3, NOS-2, heme oxygenase-1, EPO, ceruloplasmin, transferrin, transferrin receptor, IGF-binding protein-1, -2 and -3, IGF-II, TGF-B3, COX-1, aldolase A and C, phosphoglycerate kinase-1, phosphofructokinase, glucose transporters 1 and 3, hexokinase 1 and 2, glyceraldehyde-3-phosphate dehydrogenase, enolase 1, pyruvate kinase M, lactate dehydrogenase A and adenylate kinase 3. The activity of polyamide **28** in inhibiting HIF was determined in human cervical carcinoma HeLa cells. VEGF-luciferase reporter gene assay revealed that polyamide **28** inhibited the hypoxia-induced transcriptional activity of HIF in a concentration-dependent manner, and polyamide **28** reduced the iron-chelator desferrioxamine-induced expression of VEGF mRNA and secretion of VEGF protein at concentrations of 0.2 and 1 μM. In addition, real-time quantitative RT-PCR analysis showed that treatment of polyamide **28** for 48 h reduced the level of VEGF expression in a concentration-dependent manner and that ~ 60% of VEGF expression was inhibited by polyamide **28** at 1 μM.

Another patent application from Aileron Therapeutics claimed a series of peptidomimetic macrocycles as peptidic HIF inhibitors [81]. These novel peptidomimetic macrocycle compounds were designed for modulating the activity of HIF-1α through antagonization of the interaction between HIF-1α and p300–CBP transcriptional co-activators. The CAD of HIF-1α contains a region involving p300–CBP interaction. Among the highly conserved α-helices in the region, residue 796 – 805 (TSYDCEVNAP) and residue 814 – 823 (QGEELLRALD) are places that are mimicked by peptidomimetic macrocycles, such as compounds **29** and **30** (**Figure 6**). However, biological or pharmaceutical data for the claimed peptidomimetic macrocycles were not mentioned.

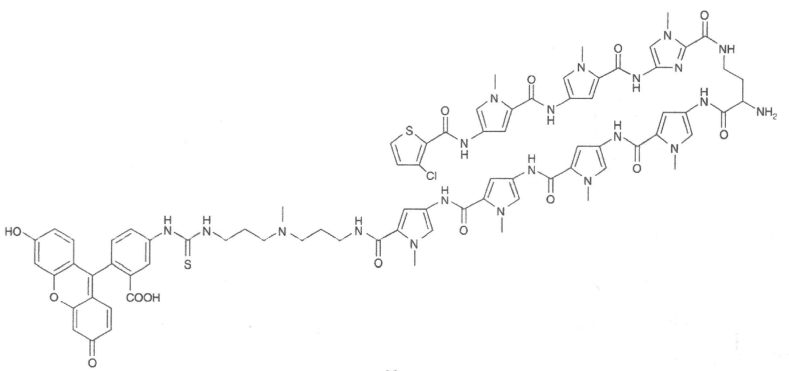

28

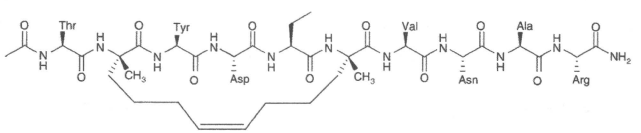

29

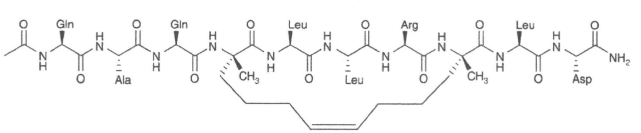

30

Figure 6. Peptic HIF inhibitors.

5. Natural product-based HIF inhibitors

5.1 Geldanamycin derivatives

Benzoquinone ansamycin antibiotic geldanamycin is a HSP90-specific inhibitor and exhibits potent anticancer activity [82]. Various geldanamycin analogs such as 17-allylaminogeldanamycin (17-AAG/tanespimycin, compound **31** in **Figure 7**), a less toxic and more stable analog, 17-allylamino-17-demethoxygeldanamycin and a water-soluble analog have been reported [83]. Interestingly, geldanamycin and its analogs exert inhibitory effects on HIF activation through the induction of proteasomal degradation of HIF-1α [84,85]. The action mechanism that has been reported indicates that tanespimycin induces the reduction of HSP90 binding to HIF-1α and leads to increased binding of receptor of activated C kinase-1, which recruits elongin C and its E3 ligase complex to HIF-1α, resulting in degradation through ubiquitin–proteasome pathway [86]. A patent application from Massachusetts Eye & Ear Infirmary claimed the use of 17-AAG for treatment of uveitis through the inhibition of HIF-1α [87]. 17-AAG suppressed lipopolysaccharide (LPS)-induced upregulation of HIF-1α in leukocytes from rats with endotoxin-induced uveitis, without affecting the expression of LPS receptor CD14. Consequently, the LPS-induced expression of VEGF was inhibited by tanespimycin.

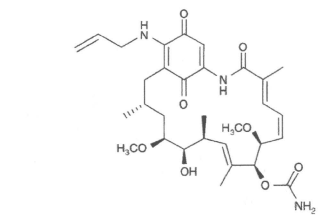

31 (Tanespimycin)

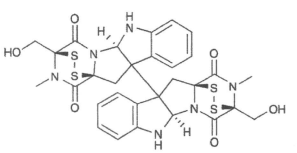

32 (Chaetocin)

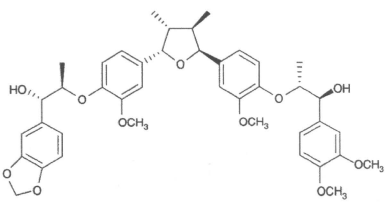

33 (Manassantin B)

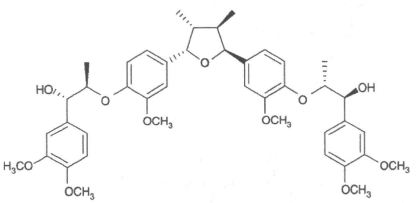

34 (Manassantin A)

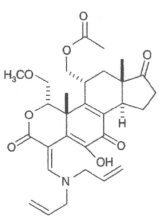

35 (PX-866)

Figure 7. Natural products and derivatives.

In Phase I clinical trials, tanespimycin was tolerated in patients even though HSP90 is present in both normal and cancer cells. Tanespimycin has a 100-fold higher binding affinity to Hsp90 in multichaperone complexes with high ATPase activity derived from tumor cells than Hsp90 in a latent uncomplexed state from normal cells [88]. A Phase II clinical study in patients with metastatic parpillary and clear cell renal cell carcinoma showed that tanespimycin did not achieve objective response in the treatment of either cohort patients [89]. Meanwhile, in a Phase II clinical trial with patients with metastatic melanoma, one of eleven patients treated with tanespimycin had SD for 6 months and median survival for all patients was 173 days. Therefore, further study of tanespimycin in melanoma is now in consideration [90]. A Phase I dose-escalation study in patients with relapsed/refractory multiple myeloma revealed that tanespimycin monotherapy was well tolerated and demonstrated activity at all tested doses (150 – 525 mg/m^2) [91].

Phase I or II clinical studies of tenespimycin in combination with other chemotherapeutic agents including sorafenib (renal cancer, melanoma) [92], bortezomib (ultiple myeloma), herceptin (Her-2 positive breast cancer) and gleevec (myelogenous leukemia) are currently under investigation.

5.2 Chaetocin

Chaetocin (compound **32** in **Figure 7**) is a thiodioxopiperazine natural product produced by *Chaetomium* species fungi and has a wide range of biologic activities, including antimicrobial, anti-inflammatory and anticancer effects [93]. In 2006, HIF inhibitor activity of chaetocin was disclosed by Cell Therapeutics Europe S.R.L. [94]. From the result of DELFIA fluorescence assay, chaetocin showed inhibition of the interaction between HIF-1α and p300 with an IC_{50} of 12.5 μM. Inhibition of VEGF expression by chaetocin was carried out using VEGF-luciferase assay and secreted VEGF ELISA assay in Hep3B, and IC_{50} values were 0.04 and 0.1 μM, respectively.

5.3 Manassantin

Manassantins and dineolignans isolated from *Saururus chinensis* are known to have various biological activities, such as neuroleptic, anti-inflammatory and ACAT inhibitory activities [95-97]. The anti-inflammatory activity of manassantins is mediated by the inhibition of NF-κB transactivation activity [98]. A patent application from the University of Mississippi disclosed the anticancer activity and HIF-inhibitory activity of manassantins [99]. Among the claimed compounds, manassantin B (compound **33** in **Figure 7**) at 10 and 100 nM completely inhibited the hypoxia-induced HIF-1α expression. Manassantin B also suppressed the hypoxic activation of HIF-1 in T47D cell-based reporter assay with an IC_{50} of 3 nM. Recently, another patent application from Duke University claimed the use of new and known manassantin derivatives as an HIF inhibitor [100]. Specifically, manassantin A (compound **34** in **Figure 7**) showed potent inhibitory activity against the hypoxia-induced HIF-1α expression at the concentration range of 1 nM to 1 μM, and a complete inhibition was observed at 100 nM.

5.4 Wartmannin derivative, PX-866

PI3K is a signal transduction enzyme that catalyzes the phosphorylation of phosphatidylinositol (4,5)-biphosphate to form phosphatidylinositol (3,4,5)-triphosphate in response to activation of receptor tyrosine kinases, GPCRs or cytokine receptors. TGF-α is a ligand for the EGFR. EGFR activates several signaling pathways including PI3K. Because EGFR activation is associated with fibroproliferative processes in human lung disease, the PI3K-Akt pathway mediates TGF-α-induced pulmonary fibrosis. PX-866 (compound **35** in **Figure 7**), a wartmannin derivative, has shown inhibition of PI3K to prevent TGF-α-induced pulmonary fibrosis [101]. Induction of lung-specific TGF-α expression in transgenic mice caused progressive pulmonary fibrosis over a 4-week period. The increase in levels of phosphorylated Akt was blocked by treatment with PX866 [102]. A Phase I clinical trial is now underway.

6. RNA antagonist, EZN-2968

EZN-2968 is a RNA antagonist composed of a third-generation oligonucleotide, locked nucleic acid, a technology that specifically binds and inhibits the expression of HIF-1α mRNA. EZN-2968 induced a potent, selective and durable antagonism of HIF-1 mRNA and protein expression (IC_{50}, 1 – 5 nM) under both normoxia and hypoxia associated with cell growth inhibition in human prostate and glioblastoma cells. Administration of EZN-2968 to normal mice led to specific, dose-dependent and highly potent downregulation of endogenous HIF-1α and VEGF in the liver. Tumor reduction was found in nude mice implanted with DU145 human prostate cancer cells treated with EZN-2968 [103-105]. A Phase I clinical study in patients with advanced malignancies revealed that EZN-2968 was well tolerated in previously treated patients. Pharmacokinetic data do not show accumulation of EZN-2968. Final results have not been reported yet [106].

7. Expert opinion

The earliest insight into the transcriptional regulation of EPO gene expression, activated by hypoxia, led to the discovery of HIF-1 and its first biochemical purification and characterization were achieved by Wang and Semenza [107]. Targeting HIF has been studied in two different therapies for the last decade: anemia caused by chronic kidney disease and neovascularization in solid tumors. HIF-1α a stabilized subunit under normoxia provides a possible approach for treatment of anemia. PHD regulates the HIF-1α subunit at the protein level in response to cellular oxygen concentration; thus, a wide variety of PHD inhibitors have been developed for erythropoiesis stimulating agents [108]. Patenting activity relating to inhibitors of neovascularization in solid tumors has increased exponentially in the last 7 years.

Although various small molecules have been developed as HIF-1 inhibitors, their inhibition mechanisms still are not clear in many cases. The most important HIF-1α regulatory systems are PI3K/Akt/mTOR, MAPK, the HSP90 system, topoisomerase I and Trx-1 [109]. Clinical trials have been carried out with several HIF-1 inhibitors, including tenaspimycin, PX-866, PX-12, EZN-2968 and PX-478 in the last 7 years. Among them, tenaspimycin has been most widely studied in clinical trials. HSP90, a target protein of tenaspimycin, is a molecular chaperone, and 48 proteins of the 280 reported Hsp90 client proteins are involved in cell growth and various signal cascades. Several client proteins are oncogenes and responsive to HSP90 inhibitors, and the most sensitive client appears to be Her2, which is followed by mutant EGFR, Raf, Akt, mutant BRAF and wild-type EGFR, in this order. Although monotherapy of tenaspimycin was not effective in patients with papillary and clear cell renal cell carcinoma [99], the strategy using tenaspimycin in combination with other chemotherapeutic agents, which target those HSP90 inhibitor-sensitive clients, is probably effective for inducing antitumor activity. In this regard, the current clinical studies of tenaspimycin in combination with other chemotherapeutic agents including sorafenib (Raf), bortezomib (proteasome), herceptin (Her-2) and gleevec (Bcr-Abl) would result in promising approaches.

Another promising approach seems to be inhibition of the PI3K/Akt/mTOR pathway, which may be effective against tumors by two distinct mechanisms, by directly blocking tumor cell growth and by inhibition tumor angeogenesis. Various PI3K inhibitors have been studied in clinical trials and the early findings suggest that the drugs are relatively well tolerated and downregulation of the pathway has been achieved [110]. However, there have been relatively few clinical responses. Signaling pathways in cancer are complex and the blocking of single pathways is not sufficient to suppress malignant growth and progression in tumors. Therefore, a combination strategy is considered to be more potent than single agent therapy.

All of the above molecules except EZN-2968 are likely to have off-target effects. EZN-2968 is a RNA antagonist targeting HIF-1α mRNA and directly inhibits HIF-1α expression. Therefore, EZN-2968 is considered to have the best potential for specific HIF-1α inhibition. Promising results of the clinical studies are expected.

High tumor HIF-1 activity is an independent predictor of poor prognosis after radiotherapy [111]. HIF-1 is upregulated in irradiated tumors and serves as a promising target for radiosensitization. Radiation causes tumor oxygenation to increase, causing, in turn, both the accumulation of tumor-reactive oxygen/nitrogen species and the depolymerization of stress granules. These two events lead to increased expression of HIF-1 and its target downstream genes. As a result, the increased expression of HIF-1-regulated cytokines delivers survival signals to tumor endothelium, resulting in tumor radioresistance through vascular radioprotection. Tumor radioresistance is predominantly mediated by tumor–stromal interactions and the capacity of a tumor to compensate for radiation-induced vascular damage through ischemic HIF-1-dependent angiogenic signaling. Inhibition of post-radiation HIF-1 signaling with PX-478 is a promising strategy to disrupt this adaptive cascade and to overcome tumor radioresistance [112].

HIF-1 induces a vast array of gene products controlling energy metabolism, neovascularization, survival, pH and cell migration for tumor growth. Nevertheless, the half-life of HIF-1α protein is only several minutes under normal oxygenated conditions. Therefore, HIF-1 is an attractive therapeutic target with great potential, and HIF inhibitor may have not only cytostatic antitumor effects with fewer side effects but also synergetic effects combined with radiotherapy.

Declaration of interest

The authors have received financial support in part by a Grant-on-Aid for scientific research on priority areas "Cancer Therapy" from the Ministry of Education, Culture, Sports, Science and Technology, Japan. They declare no other conflict of interest.

Bibliography

Papers of special note have been highlighted as either of interest (•) or of considerable interest (••) to readers.

1. Semenza GL, Wang GL. A nuclear factor induced by hypoxia via de novo protein synthesis binds to the human erythropoietin gene enhancer at a site required for transcriptional activation. Mol Cell Biol 1992;12:5447-54
2. Shweiki D, Itin A, Soffer D, et al. Vascular endothelial growth factor induced by hypoxia may mediate hypoxia-initiated angiogenesis. Nature 1992;359:843-5
3. Wang GL, Jiang BH, Rue EA, et al. Hypoxia-inducible factor-1 is a basic-helix-loop-helix-PAS heterodimer regulated by cellular O2 tension. Proc Natl Acad Sci USA 1995;92:5510-14
4. Iwai K, Yamanaka K, Kamura T, et al. Identification of the von Hippel-lindau tumor-suppressor protein as part of an active E3 ubiquitin ligase complex. Proc Natl Acad Sci USA 1999;96:12436-41
5. Maxwell PH, Wiesener MS, Chang GW, et al. The tumour suppressor protein VHL targets hypoxia-inducible factors for oxygen-dependent proteolysis. Nature 1999;399:271-5
6. Ohh M, Park CW, Ivan M, et al. Ubiquitination of hypoxia-inducible factor requires direct binding to the beta-domain of the von Hippel-Lindau protein. Nat Cell Biol 2000;2:423-7
7. Yu F, White SB, Zhao Q, et al. HIF-1alpha binding to VHL is regulated by stimulus-sensitive proline hydroxylation. Proc Natl Acad Sci USA 2001;98:9630-5
8. Cockman ME, Masson N, Mole DR, et al. Hypoxia inducible factor-alpha binding and ubiquitylation by the von Hippel-Lindau tumor suppressor protein. J Biol Chem 2000;275:25733-41
9. Kallio PJ, Wilson WJ, O'Brien S, et al. Regulation of the hypoxia-inducible transcription factor 1alpha by the ubiquitin-proteasome pathway. J Biol Chem 1999;274:6519-25
10. Berra E, Richard DE, Gothie E, et al. HIF-1-dependent transcriptional activity is required for oxygen-mediated HIF-1alpha degradation. FEBS Lett 2001;491:85-90
11. Hewitson KS, McNeill LA, Riordan MV, et al. Hypoxia-inducible factor (HIF) asparagine hydroxylase is identical to factor inhibiting HIF (FIH) and is related to the cupin structural family. J Biol Chem 2002;16:1466-71
12. Jaakkola P, Mole DR, Tian YM, et al. Targeting of HIF-alpha to the von Hippel-Lindau ubiquitylation complex by O2-regulated prolyl hydroxylation. Science 2001;292:468-72

• **Presents the mechanisms that regulate HIF-1alpha degradation by oxygen.**

13. Ivan M, Kondo K, Yang H, et al. HIFalpha targeted for VHL-mediated destruction by proline hydroxylation: implications for O2 sensing. Science 2001;292:464-8
14. Wenger RH. Cellular adaptation to hypoxia: O2-sensing protein hydroxylases, hypoxia-inducible transcription factors, and O2-regulated gene expression. FASEB J 2002;16:1151-62
15. Zhong H, De Marzo AM, Laughner E, et al. Overexpression of hypoxia-inducible factor 1alpha in

common human cancers and their metastases. Cancer Res 1999;59:5830-5

• **Describes the *in vivo* experiments that validate HIF as a target for cancer.**

16. Folkman J. Angiogenesis: an organizing principle for drug discovery? Nat Rev Drug Discov 2007;6:273-86

17. Pouyssegur J, Dayan F, Mazure NM. Hypoxia signalling in cancer and approaches to enforce tumour regression. Nature 2006;441:437-43

•• **Highlights the features of hypoxia signaling.**

18. Bertout JA, Patel SA, Simon MC. The impact of O2 availability on human cancer. Nat Rev Cancer 2008;8:967-75

19. Semenza GL. Targeting HIF-1 for cancer therapy. Nat Rev Cancer 2003;3:721-32

•• **Reviews the potential of HIF-1 as a therapeutic target in cancer.**

20. Kirkpatrick DL, Kuperus M, Dowdeswell M, et al. Mechanisms of inhibition of the thioredoxin growth factor system by antitumor 2-imidazolyl disulfides. Biochem Pharmacol 1998;55:987-94

21. Welsh SJ, Williams RR, Birmingham A, et al. The thioredoxin redox inhibitors1-methylpropyl 2-imidazolyl disulfide and pleurotin inhibit hypoxia-induced factor 1a and vascular endothelial growth factor formation. Mol Cancer Ther 2003;2:235-43

22. Ramanathan RK, Kirkpatrick DL, Belani CP, et al. A phase 1 pharmacokinetic and pharmacodynamic study of PX-12, a novel inhibitor of thioredoxin-1, in patients with advanced solid tumors. Clin Cancer Res 2007;13:2109-14

23. ProlX Pharmaceuticals. Compositions and methods for using asymmetric disulfides. WO082686; 2009

24. Ramanathan RK, Abbruzzese J, Dragovich T, et al. A randomized phase II study of PX-12, an inhibitor of thioredoxin in patients with advanced cancer of the pancreas following progression after a gemcitabine-containing combination. Cancer Chemother Pharmacol 12 May 2010. [Epub ahead of print] DOI: 10.1007/s00280-010-1343-8

25. Welsh S, Williams R, Kirkpatrick L, et al. Antitumor activity and pharmacodynamic properties of PX-478, an inhibitor of hypoxia-inducible factor-1alpha. Mol Cancer Ther 2004;3:233-44

26. ProlX Pharmaceuticals. N-Oxides and derivatives of melphalan for treating diseased states associated with hypoxia inducible factor. WO043359; 2004

27. ProlX Pharmaceuticals. Regulation of HIF protein levels via deubiquitinatio pathways. WO007828; 2005

28. Ravi R, Mookerjee B, Bhujwalla ZM, et al. Regulation of tumor angiogenesis by p53-induced degradation of hypoxia-inducible factor 1alpha. Genes Dev 2000;14:34-44

29. ProlX Pharmaceuticals. Method of pre-selecting patients for anti-VEGF, anti-HIF-1 or anti-thioredoxin therapy. WO023658; 2006

30. Board of regents of the University of Texas System. Compositions and methods for treating lung cancer. WO102960; 2009

31. Tibes R, Falchook GS, Von Hoff DD, et al. Results from a phase I, dose-escalation study of PX-478, an orally available inhibitor of HIF-1alpha. J Clin Oncol 2010;28(Suppl):3076

32. Teng CM, Wu CC, Ko FN, et al. YC-1, a nitric oxide-independent activator of soluble guanylate cyclase, inhibits platelet-rich thrombosis in mice. Eur J Pharmacol 1997;320:161-6

33. Galle J, Zabel U, Hubner U, et al. Effects of the soluble guanylyl cyclase activator, YC-1, on vascular tone, cyclic GMP levels and phosphodiesterase activity. Br J Pharmacol 1999;127:195-203

34. Chun YS, Yeo EJ, Choi E, et al. Inhibitory effect of YC-1 on the hypoxic induction of erythropoietin and vascular endothelial growth factor in Hep3B cells. Biochem Pharmacol 2001;61:947-54

35. Hif Bio, Inc. Method for inhibiting tumor angiogenesis and tumor growth. WO091648; 2004

36. Hif Bio, Inc. Compounds, compositions and methods. WO030121; 2005

37. Hif Bio, Inc. Anti-angiogenesis compounds. WO065010; 2007

38. Emory University and Scripps Research Institute. HIF-1 inhibitors. WO087066; 2004

39. Emory University and Scripps Research Institute. HIF inhibitors. WO025169; 2007

40. Nicolaou KC, Pfefferkorn JA, Roecker, AJ, et al. Natural product-like combinatorial libraries based on privileged structures. 1. General principles and solid-phase synthesis of benzopyrans. J Am Chem Soc 2000;122:9939-53

41. Nicolaou KC, Pfefferkorn JA, Mitchell HJ, et al. Natural product-like combinatorial libraries based on privileged structures. 2. Construction of a 10000-membered benzopyran library by directed split-and-pool chemistry using NanoKans and optical encoding. J Am Chem Soc 2000;122:9954-67

42. Nicolaou KC, Pfefferkorn JA, Barluenga S, et al. Natural Product-like Combinatorial Libraries based on privileged structures. 3. The 'Libraries from Libraries' Principle for diversity enhancement of benzopyran libraries. J Am Chem Soc 2000;122:9968-76

43. Emory University. Small molecule inhibitors of HIF and angiogenesis. WO006184; 2010

44. Emory University and Scripps Research Institute. Small molecule inhibitors of HIF and angiogenesis. WO006189; 2010

45. National Cancer Institute. Tricyclic compounds as inhibitors of the hypoxic signal pathway. WO118580; 2005

46. Lee HH, Palmer BD, Boyd M, et al. Potential antitumor agents. 64. Synthesis and antitumor evaluation of dibenzo1,4] dioxin-1-carboxamides: a new class of weakly binding DNA-intercalating agents. J Med Chem 1992;35:258-66

47. Creighton-Gutteridge M, Cardellina JH II, Stephen AG, et al. Cell type-specific, topoisomerase II-dependent inhibition of hypoxia-inducible factor-1alpha protein accumulation by NSC 644221. Clin Cancer Res 2007;13:1010-18

48. Cell TherapeuticsEuro S.R.L. Use of thiazolidinone derivatives as antiangiogenic agents. WO066846; 2006

49. University of Texas. Compositions and methods for inhibition of tyrosine kinases. WO030795; 2008

50. Piramal Life Sciences Ltd. Pyridyl derivatives, their preparation and use. WO019656; 2009

51. Yewalkar N, Deore V, Padgaonkar A, et al. Development of novel inhibitors targeting HIF-1alpha towards anticancer drug discovery. Bioorg Med Chem Lett 2010;20:6426-9

52. Noguchi T, Fujimoto H, Sano H, et al. Angiogenesis inhibitors derived from thalidomide. Bioorg Med Chem Lett 2005;15:5509-13

53. Charlesson LLC. Thalidomide analogs for treating vascular abnormalities. WO154353; 2008

54. Charlesson LLC homepage. Available from: http://www.charlessonllc.com/index.html

55. Bayer Schering Pharma AG. Heteroaryl substituted pyrazole derivatives useful for treating hyper-proliferative disorders and diseases associated with angiogenesis. WO141731; 2008

56. Bayer Schering Pharma AG. Aminoalkyl-substituted compounds as HIF inhibitors. WO054762; 2010

57. Bayer Schering Pharma AG. Heterocyclically substituted aryl compounds as HIF inhibitors. WO054763; 2010

58. Bayer Schering Pharma AG. Heteroaromatic compounds for use as HIF inhibitors. WO054764; 2010

59. Korea Research Institute of Bioscience and Biotechnology. Compounds that inhibit HIF-1 activity, the method for preparation thereof and the pharmaceutical composition containing them as an effective component. WO004798; 2008

60. Lee K, Kang JE, Park SK, et al. LW6, a novel HIF-1 inhibitor, promotes proteasomal degradation of HIF-1alpha via upregulation of VHL in a colon cancer cell line. Biochem Pharmacol 2010;80:982-9

61. Lee K, Lee JH, Boovanahalli SK, et al. (Aryloxyacetylamino)benzoic acid analogues: A new class of hypoxia-inducible factor-1 inhibitors. J Med Chem 2007;50:1675-84

62. Won MS, Im N, Park S, et al. A novel benzimidazole analogue inhibits the hypoxia-inducible factor (HIF)-1 pathway. Biochem Biophys Res Commun 2009;385:16-21

63. Shimizu K, Maruyama M, Yasui Y, et al. Boron-containing phenoxyacetanilide derivatives as hypoxia-inducible factor (HIF)-1alpha inhibitors. Bioorg Med Chem Lett 2010;20:1453-6

64. Ban HS, Shimizu K, Minegishi H, et al. Identification of HSP60 as a primary target of o-carboranylphenoxyacetanilide, an HIF-1alpha inhibitor. J Am Chem Soc 2010;132:11870-1

65. Centro de Investigacion Principe Felipe. Pharmaceutical composition for inhibiting the transcription factor inducible by hypoxia, modulators of pathological processes of angiogenesis, oncogenesis, inflammation, apoptosis, and cellular therapy. WO112615; 2009

66. Moreno-Manzano V, Rodríguez-Jimenez FJ, Acena-Bonilla JL, et al. FM19G11, a new hypoxia-inducible factor (HIF) modulator, affects stem cell differentiation status. J Biol Chem 2010;285:1333-42

67. Rodriguez-Jimenez FJ, Moreno-Manzano V, Mateos-Gregorio P, FM19G11: a new modulator of HIF that links mTOR activation with the DNA damage checkpoint pathways. Cell Cycle 2010;9:2803-13

68. Threshold Pharmaceuticals. Combination therapies for the treatment of cancer. WO064734; 2004

69. Cell Therapeutics Europe S.R.L. Indole derivatives with antitumor activity. WO066923; 2006

70. Bionaut Pharmaceuticals. Anti-neoplastic agents, combination therapies and related methods. WO060951; 2005

71. Bionaut Pharmaceuticals. Pancreatic cancer treatment using Na+/K+ ATPase inhibitors. WO028969; 2006

72. Bionaut Pharmaceuticals. Treatments of refractory cancers using Na+/K+ ATPase inhibitors. WO029020; 2006

73. Bionaut Pharmaceuticals. Combinatorial chemotherapy treatment using Na+/K+ ATPase inhibitors. WO029018; 2006

74. Bionaut Pharmaceuticals. Use of Na+/K+ ATPase inhibitors and antagonists thereof. WO044916; 2006

75. Bionaut Pharmaceuticals. Modulators of hypoxia inducible factor-1 and related uses for the treatment of ocular disorders. WO016656; 2007

76. Btg International. Modulators of hypoxia inducible factor-1 and related uses. WO081835; 2007

77. Btg International. Modulators of hypoxia inducible factor-1 and related uses. WO093086; 2008

78. Sri International. Method and composition for inhibiting cell proliferation and angiogenesis. WO113842; 2006

79. Duellman SJ, Calaoagan JM, Sato BG, et al. A novel steroidal inhibitor of estrogen-related receptor alpha (ERRalpha). Biochem Pharmacol 2010;80:819-26

80. California Institute of Technology. Compositions and methods for inhibiting expression of hypoxia-inducible genes. WO120582; 2005

81. Aileron Therapeutics. Peptidomimetic macrocycles. WO034028; 2010

82. Whitesell L, Mimnaugh EG, De Costa B, et al. Inhibition of heat shock protein HSP90-pp60v-src heteroprotein complex formation by benzoquinone ansamycins: essential role for stress proteins in oncogenic transformation. Proc Natl Acad Sci USA 1994;91:8324-8

83. Kaur G, Belotti D, Burger AM, et al. Antiangiogenic properties of 17-(dimethylaminoethylamino)-17-demethoxygeldanamycin: an orally bioavailable heat shock protein 90 modulator. Clin Cancer Res 2004;10:4813-21

84. Mabjeesh NJ, Post DE, Willard MT, et al. Geldanamycin induces degradation of hypoxia-inducible factor 1alpha protein via the proteosome pathway in prostate cancer cells. Cancer Res 2002;62:2478-82

85. Isaacs JS, Jung YJ, Mimnaugh EG, et al. Hsp90 regulates a von Hippel Lindau-independent hypoxia-inducible factor-1alpha-degradative pathway. J Biol Chem 2002;277:29936-44

86. Liu YV, Baek JH, Zhang H, et al. RACK1 competes with HSP90 for binding to HIF-1alpha and is required for O2-independent and

HSP90 inhibitor-induced degradation of HIF-1alpha. Mol Cell 2007;25:207-17

87. Massachusetts Eye & Ear Infirmary. Inflammatory eye disease. WO105077; 2005

88. Kamal A, Thao L, Sensintaffar J, et al. A high-affinity conformation of Hsp90 confers tumour selectivity on Hsp90 inhibitors. Nature 2003;425:407-10

89. Ronnen EA, Kondagunta GV, Ishill N, et al. A phase II trial of 17-(Allylamino)-17-demethoxygeldanamycin in patients with papillary and clear cell renal cell carcinoma. Invest New Drugs 2006;24:543-6

90. Pacey S, Gore M, Chao D, et al. A Phase II trial of 17-allylamino, 17-demethoxygeldanamycin (17-AAG, tanespimycin) in patients with metastatic melanoma. Invest New Drugs 5 Aug 2010. [Epub ahead of print] DOI: 10.1007/s10637-010-9493-4

91. Richardson PG, Chanan-Khan AA, Alsina M, et al. Tanespimycin monotherapy in relapsed multiple myeloma: results of a phase 1 dose-escalation study. Br J Haematology 2010;150:438-45

92. Vaishampayan UN, Burger AM, Sausville EA, et al. Safery, efficacy, pharmacokinetics, and pharmacodynamics of the combination of sorafenib and tanespimycin. Clin Cancer Res 2010;16:3795-804

93. Isham CR, Tibodeau JD, Jin W, et al. Chaetocin: a promising new antimyeloma agent with in vitro and in vivo activity mediated via imposition of oxidative stress. Blood 2007;109:2579-88

94. Cell Therapeutics Europe S.R.L. Use of diketodithiopiperazine antibiotics for the preparation of antiangiogenic pharmaceutical compositions. WO066775; 2006

95. Rao KV, Puri VN, Diwan PK, et al. Preliminary evaluation of manassantin A, a potential neuroleptic agent from Saururus cernuus. Pharmacol Res Commun 1987;19:629-38

96. Hwang BY, Lee J-H, Nam JB, et al. Lignans from Saururus chinensis inhibiting the transcription factor NF-kappaB. Phytochemistry 2003;64:765-71

97. Lee WS, Lee D-W, Baek Y-I, et al. Human ACAT-1 and -2 inhibitory activities of saucerneol B, manassantin A and B isolated from Saururus chinensis. Bioorg Med Chem Lett 2004;14:3109-12

98. Lee JH, Hwang BY, Kim KS, et al. Suppression of RelA/p65 transactivation activity by a lignoid manassantin isolated from Saururus chinensis. Biochem Pharmacol 2003;66:1925-33

99. The University of Mississippi. Saururus cernuus compounds that inhibit cellular responses to hypoxia. WO110348; 2004

100. Duke University. Manassantin compounds and methods of making and using same. WO059858; 2010

101. University of Arizona. Wortmannin analogs and methods using same. WO024183; 2003

102. Le Cras TD, Korfhagen TR, Davidson C, et al. Inhibition of PI3K by PX-866 prevents transforming growth factor-alpha-induced pulmonary fibrosis. Am J Pathology 2010;176:679-86

103. Enzon Pharmaceuticals, Inc. Potent LNA oligonucleotides for the inhibition of HIF-1a expression. WO0286859; 2009

104. Enzon Pharmaceuticals, Inc. Oligomeric compounds for the modulation of HIF-1alpha expression. WO0093839; 2010

105. Greenberger LM, Horak ID, Filpula D, et al. A RNA antagonist of hypoxia-inducible factor-1alpha. EZN-2968, inhibits tumor cell growth. Mol Cancer Thr 2008;7:3598-608

106. Patnaik A, Chiorean EG, Tolcher A, et al. EZN-2968, anovel hypoxia-inducible factor-1alpha (HIF-1alpha) messanger ribonucleic acid (mRNA) antagonist: results of a phase I, pharmacokinetics (PK), dose-escalation study of daily administration in patients (pts) with advanced malignancies. J Clin Oncol 2009;27:abstract 2564

107. Wang GL, Semenza GL. Purification and characterization of hypoxia-inducible factor 1. J Biol Chem 1995;270:1230-7

108. Yan L, Colandrea VJ, Hale JJ, Prolyl hydroxylase domain-containing protein inhibitors as stabilizers of hypoxia-inducible factor: small molecule-based therapeutics for anemia. Expert Opin Ther Patients 2010;20;1219-45

109. Diaz-Gonzalez JA, Russell J, Rouzaut A, et al. Targeting hypoxia and angiogenesis through HIF-1alpha inhibition. Cancer Biol Ther 2005;4:1055-62

110. Liu P, Cheng H, Roberts, TM, et al. Targeting the phosphoinositide 3-kinase pathway in cancer. Nat Rev Drug Discov 2009;8:627-44

111. Aebersold DM, Burri P, Beer KT, et al. Expression of hypoxia-inducible factor-1alpha: a novel predictive and prognostic parameter in the radiotherapy of oropharyngeal cancer. Cancer Res 2001;61:2911-16

112. Schwartz DL, Powis G, Thitai-Kumar A, et al. The selective hypoxia inducible factor-1 inhibitor PX-478 provides in vivo radiosensitization through tumor stromal effects. Mol Cancer Ther 2009;8:947-58

Affiliation

Hyun Seung Ban[1] PhD, Yoshikazu Uto[2] PhD & Hiroyuki Nakamura[†3] PhD
[†]Author for correspondence
[1]Gakushuin University,
Department of Chemistry,
Faculty of Science,
1-5-1, Mejiro, Toshima-ku,
Tokyo, 171-8588, Japan
[2]Medicinal Chemistry Research Lab.
Sankyo Co., Ltd.,
1-2-58, Hiromachi,
Shinagawa-ku, Tokyo,
140-8710, Japan
[3]Professor,
Gakushuin University,
Department of Chemistry,
Faculty of Science,
1-5-1, Mejiro,
Toshima-ku, Tokyo,
171-8588, Japan
Tel: +81 3 3986 0221;
Fax: +81 3 5992 1029;
E-mail: hiroyuki.nakamura@gakushuin.ac.jp

TISSUE ENGINEERING: Part C
Volume 17, Number 2, 2011

DOI: 10.1089/ten.tec.2010.0139

Transplantation of Human Adipose Tissue-Derived Multilineage Progenitor Cells Reduces Serum Cholesterol in Hyperlipidemic Watanabe Rabbits

Hanayuki Okura, Ph.D.,[1,2] Ayami Saga, M.S.,[1] Yuichi Fumimoto, M.D., Ph.D.,[1] Mayumi Soeda, V.M.D.,[1] Mariko Moriyama, Ph.D.,[1,3] Hiroyuki Moriyama, Ph.D.,[3] Koji Nagai, M.D.,[1,4] Chun-Man Lee, M.D., Ph.D.,[1] Shizuya Yamashita, M.D., Ph.D.,[5] Akihiro Ichinose, M.D., Ph.D.,[4] Takao Hayakawa, Ph.D.,[3] and Akifumi Matsuyama, M.D., Ph.D.[1]

Familial hypercholesterolemia (FH) is an autosomal codominant disease characterized by high concentrations of proatherogenic lipoproteins and premature atherosclerosis secondary to low-density lipoprotein (LDL) receptor deficiency. We examined a novel cell therapy strategy for the treatment of FH in the Watanabe heritable hyperlipidemic (WHHL) rabbit, an animal model for homozygous FH. We delivered human adipose tissue-derived multilineage progenitor cells (hADMPCs) via portal vein and followed by immunosuppressive regimen to avoid xenogenic rejection. Transplantation of hADMPCs resulted in significant reductions in total cholesterol, and the reductions were observed within 4 weeks and maintained for 12 weeks. ^{125}I-LDL turnover study showed that the rate of LDL clearance was significantly higher in the WHHL rabbits with transplanted hADMPCs than those without transplanted. After transplantation hADMPCs were localized in the portal triad, subsequently integrated into the hepatic parenchyma. The integrated cells expressed human albumin, human alpha-1-antitrypsin, human Factor IX, human LDL receptors, and human bile salt export pump, indicating that the transplanted hADMPCs resided, survived, and showed hepatocytic differentiation *in vivo* and lowered serum cholesterol in the WHHL rabbits. These results suggested that hADMPC transplantation could correct the metabolic defects and be a novel therapy for inherited liver diseases.

Introduction

Familial hypercholesterolemia (FH) is characterized by premature and accelerated development of atherosclerotic lesions caused by elevated levels of cholesterol-rich lipoproteins in plasma. The disease is caused by mutations in the low-density lipoprotein (LDL) receptor gene that result in a significant decrease in receptor-mediated uptake of lipoproteins from the circulation.[1–3] Patients homozygous for defects in LDL receptors have serum cholesterol levels 5–10 times those of normal and suffer as early as the first two decades of life from complications such as coronary artery disease.[4,5] In homozygous FH patients, conventional drug therapy cannot treat the condition, and therapeutic recourses are limited to chronic plasmapheresis or orthotopic liver transplantation.[1] Although liver transplants lower LDL levels, the procedure is life threatening; in addition, donor livers are in short supply. Cellular transplantation has been proposed to provide functional LDL receptors for the treatment of hypercholesterolemia. Transplantation of allogenic and xenogenic hepatocytes has been shown to be effective in lowering serum cholesterol in the Watanabe heritable hyperlipidemic (WHHL) rabbit,[6–9] which is an animal model for homozygous FH. Further, a number of gene therapy approaches have shown some promises in animal models and human,[10–13] and the therapies will cure a number of patients with FH in near future. As an alternative to whole-organ transplantation and/or gene therapy, we have investigated the ability of human adipose tissue-derived multilineage progenitor cells (hADMPCs) to differentiate into hepatocytes *in vitro* and to replace critical liver functions[14] as well as previous reports,[15,16] because the *in vitro* differentiation of hADMPCs into various kinds of cell types in now well reported and hADMPCs can be easily and safely obtained in large

[1]Department of Somatic Stem Cell Therapy and Health Policy, Foundation for Biomedical Research and Innovation, Kobe, Japan.
[2]Research Fellow of the Japan Society for the Promotion of Science, Tokyo, Japan.
[3]Pharmaceutical Research and Technology Institute, Kinki University, Osaka, Japan.
[4]Department of Plastic Surgery, Kobe University Hospital, Kobe, Japan.
[5]Division of Cardiology, Department of Internal Medicine, Osaka University Graduate School of Medicine, Osaka Japan.

quantities without serious ethics issues.[17,18] In this study, we are investigating whether hADMPCs could differentiate into hepatocytes *in vivo* and replace critical liver functions as considerable therapeutic potential for cellular replacement.

Materials and Methods

Cells

hADMPCs were prepared as described previously[19] with some modifications.[14,17,18] Adipose tissues from human subjects were resected during plastic surgery in five subjects (four males and one female, age, 20–60 years) as excess discards. Ten to 50 g of subcutaneous adipose tissue was collected from each subject. All subjects provided informed consent. The protocol was approved by the Review Board for Human Research of Kobe University Graduate School of Medicine, Osaka University Graduate School of Medicine, and Foundation for Biomedical Research and Innovation. After five to six passages, the hADMPCs were used for transplantation. Human cryopreserved hepatocytes were purchased from Invitrogen (Lot number: HuP81) and cultured as indicated by the manufacturer's protocol. Human adipose tissue-derived fibroblastic cells were obtained according to previous report.[20]

Flow cytometric analysis

hADMPCs isolated from adipose tissue were characterized by flow cytometry. Cells were detached from culture dishes by 0.25% trypsin/ethylenediaminetetraacetic acid (EDTA) and suspended in Dulbecco's phosphate-buffered saline (DPBS; Nacalai Tesque) containing 0.1% fetal bovine serum. Aliquots (5×10^5 cells) were incubated for 30 min at 4°C with fluorescein isothiocyanate-conjugated mouse monoclonal antibodies to human CD31 (BD PharMingen), CD105 (Ancell Corporation), CD133 (R&D Systems), phycoerythrin-conjugated mouse monoclonal antibodies to human CD29, CD34, CD45, CD73 (BD PharMingen), CD44, or CD166 (Ancell). Isotype-identical antibodies served as controls. Further, the cells were incubated with mouse monoclonal antibodies against human stage-specific embryonic antigen-4 (from Chemicon International, Inc.), ABCG-2, or CD117 (BD PharMingen) with nonspecific mouse antibody used as a negative control. After washing with DPBS, cells were incubated with phycoerythrin-labeled goat anti-mouse Ig antibody (BD PharMingen) for 30 min at 4°C. After three washes, cells were resuspended in DPBS and analyzed by flow cytometry using a FACSCalibur flow cytometer and CellQuest Pro software (BD Biosciences).

Adipogenic, osteogenic, and chondrogenic differentiation procedure

For adipogenic differentiation, cells were cultured in the differentiation medium (Zen-Bio, Inc.). After 3 days, half of the medium was changed with adipocyte medium (Zen-Bio) every 2 days. Five days after differentiation, adipocytes were characterized by microscopic observation of intracellular lipid droplets by Oil Red O staining. Osteogenic differentiation was induced by culturing the cells in Dulbecco's modified Eagle's medium containing 10 nM dexamethasone, 50 mg/dL ascorbic acid 2-phosphate, 10 mM β-glycerophosphate (Sigma), and 10% fetal bovine serum. Differentiation was examined by Alizarin red staining. For Alizarin red staining, the cells were washed three times and fixed with dehydrated ethanol. After fixation, the cells were stained with 1% Alizarin red S in 0.1% NH_4OH (pH 6.5) for 5 min and then washed with H_2O. For chondrogenic differentiation, hADMPCs were first trypsinized and 2×10^5 cells were centrifuged at 400 *g* for 10 min. The resulting pellets were cultured in the chondrogenic medium (alpha-minimum essential medium (alpha-MEM) supplemented with 10 ng/mL transforming growth factor-β, 10 nM dexamethasone, 100 μM ascorbate, and 10 μL/mL 100×ITS Solution) for 14 days. For Alcian Blue staining, nuclear counterstaining with Weigert's hematoxylin was followed by 0.5% Alcian Blue 8GX for proteoglycan-rich cartilage matrix.

hADMPC transplantation and immunosuppression regimen

WHHL rabbits (8 weeks old; purchased from Kitayama-labes, Inc.) were anesthetized with pentobarbital (50 mg/kg). An incision distal and parallel to the lower end of the ribcage was made. The peritoneum was incised, and hADMPCs ($n=5$) or human adipose tissue-derived fibroblastic cells ($n=3$) (3×10^7 cells) suspended in 3 mL of Hanks' balanced salt solutions (HBSS) (20°C) or 3 mL of control saline ($n=6$) were infused in 5 min into the portal vein via a 18-gauge Angiocath™ (BD). The immunosuppression regimen (Fig. 1A) consisted of the following: (1) intramuscular injection of cyclosporin A (6 mg/kg/day) daily from the day before surgery to sacrifice; (2) intramuscular injection of rapamycin (0.05 mg/kg/day) daily from the day before surgery to sacrifice; (3) methylprednisolone at 3 mg/kg/day (days 1–7), followed by tapering to 2 mg/kg/day (days 8–14), 1 mg/kg/day (days 15–21) and 0.5 mg/kg/day (day 22 to the time at sacrifice); (4) intravenous injection of cyclophosphamide (20 mg/kg/day) at days 0, 2, 5, and 7; (5) ganciclovir (2.5 mg/kg/day intramuscular injection (i.m.)) was also administrated to avoid viral infection in the immunocompromised host.

DNA extraction and quantification of human-derived cells

Total DNA of WHHL rabbit liver, which was obtained at the time just after hADMPC transplantation, and 2, 4, 8, and 12 weeks after transplantation, were isolated using a NucleoSpin Tissue kit (Macherey-Nagel) according to the manufacturer's instructions. hADMPCs and rabbit hepatocytes were mixed at the ratios of 100:0 (100%), 10:90 (10%), 1:99 (1%), 0.1:99.9 (0.1%), 0.01:99.99 (0.01%), and 0.001:99.999 (0.001%), and DNA was isolated. Seven hundred nanograms of each samples of extracted DNA was quantified by real-time polymerase chain reaction (PCR) using the ABI Prism 7900 Sequence Detection System (Applied Biosystems), primers for the 82 bp *Alu* amplicon (forward, 5′-GTCAGGAGATCGA GACCATCCC; reverse, 5′-CCACTACGCCCGGCTAATTT), and SYBR Green (TOYOBO) dye using a previously published protocol.[21,22] Reactions were performed in quadruplicate and the *Alu* levels were calculated by the standard curve.

Assay for lipid profiling

Serum samples were obtained from nonfasting rabbits before and after transplantation. Serum total cholesterol was measured in each sample using assay kits from Wako Pure Chemical Industries. Serum lipoproteins were analyzed by an on-line dual enzymatic method for simultaneous quantification of cholesterol and triglycerides by high-performance

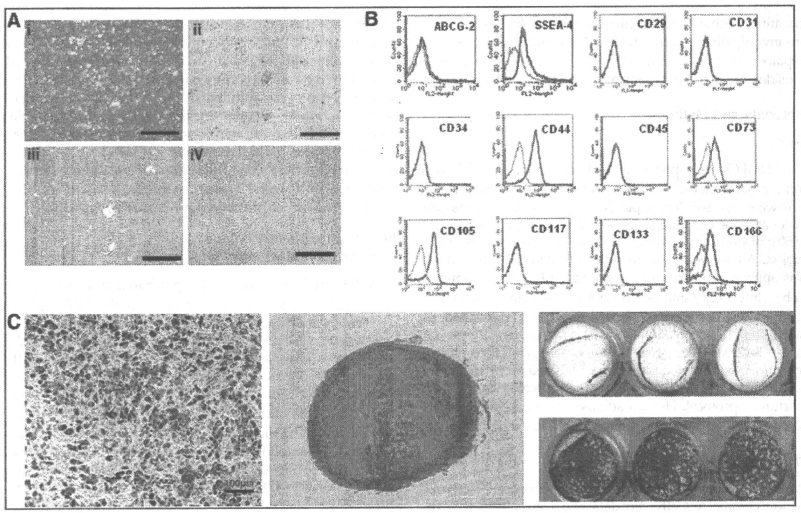

FIG. 1. **(A)** Morphological characters of human adipose tissue-derived multilineage progenitor cells (hADMPCs). The cells obtained from adipose tissue were seeded and incubated for 24 h **(i)**. After incubation, the adherent cells were treated with ethylenediaminetetraacetic acid solution, and the resulting suspended cells were replated at a density of 10,000 cells/cm^2 on human fibronectin-coated dishes (BD BioCoat) **(ii, iii)**. Within two to three passages after the initial plating of the primary culture, hADMPCs appeared as a monolayer of large flat cells (25–30 μm in diameter). As the cells approached confluence, they assumed a more spindle-shaped, fibroblastic morphology **(iv)**. i) Bar = 499 μm, ii) bar = 201 μm, iii) bar = 502 μm and iv) bar = 202 μm. **(B)** Cell surface markers expressed on hADMPCs. The cells were negative for markers of the hematopoietic lineage (CD45) and of hematopoietic stem cells, ABCG-2, CD34, and CD133. They were also negative for CD31, an endothelial cell-associated marker, and the surface antigen c-Kit (CD117). However, they stained positively for a number of surface markers characteristic of mesenchymal and/or neural stem cells, but not embryonic stem (ES) cells, including CD29, CD44 (hyaluronan receptor), CD73, CD105 (endoglin), and CD166. hADMPCs also were positive for stage-specific embryonic antigen (SSEA)-4. **(C)** Adipocytic, chondrocytic, and osteocytic differentiation potentials of hADMPCs. Adipocytic differentiation potential of hADMPCs was confirmed by Oil Red O staining (the left panel) (bar = 100 μm). Chondrocytic differentiation potential of hADMPCs was estimated by extracellular matrices with Alcian Blue staining (the middle panel). Osteogenic differentiation potential of hADMPCs was confirmed by Alizarin red S staining for mineralized nodules (the right panel).

liquid chromatography at Skylight Biotech, according to the procedure as described.[23]

Immunohistochemical staining of WHHL rabbit liver sections

The WHHL livers were harvested and fixed immediately with 10% formalin. They were placed into optimal cutting temperature compound (Sakura Finetechnical Co.), frozen immediately, and then sectioned at 7 μm thickness. The sections were then incubated with blocking solution (Blocking one; Nacalai Tesque) for 1 h. The samples were incubated with rabbit anti-human-specific albumin antibody (MBL), rabbit anti-human-specific alpha 1 anti-trypsin antibody, and rabbit anti-LDL receptor antibody, followed by Alexa Fluor 488-labeled goat anti-rabbit IgG (Molecular Probes). To show the colocalization of human CD90 and albumin, the samples were incubated with the rabbit anti-human CD90 monoclonal antibody (Epitomics, Inc.) and then with Alexa Fluor 488-labeled goat anti-rabbit IgG (Molecular Probes), and washed extensively. Then, the specimens were incubated with rabbit anti-human-specific albumin antibody (MBL), followed by Alexa Fluor 546-labeled goat anti-rabbit IgG (Molecular Probes). The treated sample was examined with a BioZero laser scanning microscope (Keyence).

PCR analysis of WHHL rabbit liver for human liver-specific genes

Total RNAs of WHHL rabbit liver, hADMPCs, and human hepatocytes were isolated using an RNAeasy kit (Qiagen). After treatment with DNase, the cDNA was synthesized using Superscript III RNase H-minus Reverse Transcriptase (Invitrogen). Real-time PCR was performed using the ABI Prism 7900 Sequence Detection System (Applied Biosystems). About 20×Assays-on-Demand™ Gene Expression Assay Mix for human alpha-1-antitrypsin (Hs01097800_m1), human albumin (Hs00609411_m1), human factor 9, human GATA-binding

protein 4 (GATA4) (Hs00171403_m1), human hepatocyte nuclear factor 3 beta (Hs00232764_m1), human LDL receptor (Hs00181192_m1), and human glyceraldehyde-3-phosphate dehydrogenase (Hs99999905_m1) were obtained from Applied Biosystems. It was confirmed that human detectors and rabbit detectors do not cross-react with the other species. TaqMan® Universal PCR Master Mix, No AmpErase® UNG (2×), was also purchased from Applied Biosystems. Reactions were performed in quadruplicate and the mRNA levels were normalized relative to human glyceraldehyde-3-phosphate dehy-

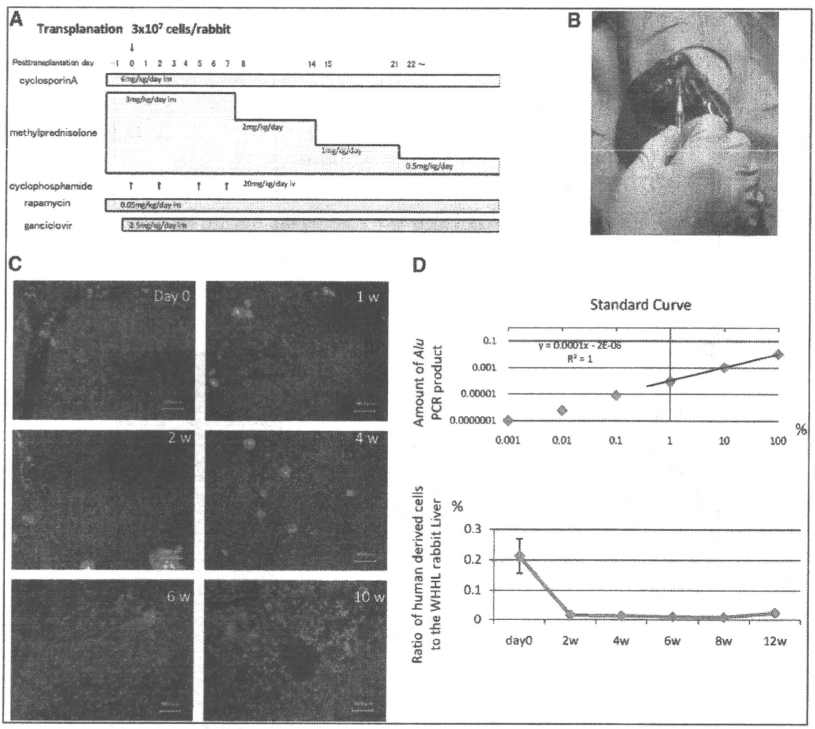

FIG. 2. **(A)** Immunosuppression regimen. Cyclosporin A (6 mg/kg/day) and rapamycin (0.05 mg/kg/day) were administered intramuscularly daily from the day before surgery to sacrifice. Methylprednisolone was administered at 3 mg/kg/day (days 1–7), 2 mg/kg/day (days 8–14), 1 mg/kg/day (days 15–21), and 0.5 mg/kg/day (day 22 to sacrifice). Cyclophosphamide (20 mg/kg/day) was injected intravenously at days 0, 2, 5, and 7. Ganciclovir (2.5 mg/kg/day) was also injected intramuscularly to avoid viral infection in the immunocompromised host. **(B)** Surgical procedure. Watanabe heritable hyperlipidemic (WHHL) rabbits were anesthetized with pentobarbital. An incision was made distal and parallel to the lower end of the ribcage. The peritoneum was incised and hADMPCs, and human adipose tissue-derived fibroblastic cells (hADFCs) (3×10^7 cells/rabbit) or controls were infused into the portal vein using an 18-gauge Angiocath. **(C)** Localization of transplanted hADMPCs in the WHHL liver. At the day of and 1, 2, 4, 6, and 10 weeks after transplantation of DiI-labeled hADMPCs via the portal vein, the WHHL rabbit liver was examined histologically. DiI-fluorescent labeled-hADMPCs resided and distributed in the portal area at the day of transplantation. One to 2 weeks after transplantation, the DiI-stained hADMPCs-derived cells were localized near the portal areas. Four weeks after transplantation some of the DiI-stained cells resembled innate hepatocytes morphologically. Six and 10 weeks after transplantation, DiI-positive transplanted cells were dispersed in a centrilobular direction, resembling the mature innate hepatocytes. Bars = 100 μm. **(D)** Quantification of repopulation of the transplanted cells in the liver. The ratios of human-derived cell repopulation were examined by analyzing an *Alu* repetitive DNA sequence at the day of and 2, 4, 8, and 12 weeks after transplantation. In upper panel the standard curve was indicated, and in lower panel the ratio of repopulation of human cells was shown in time course after transplantation of hADMPCs.

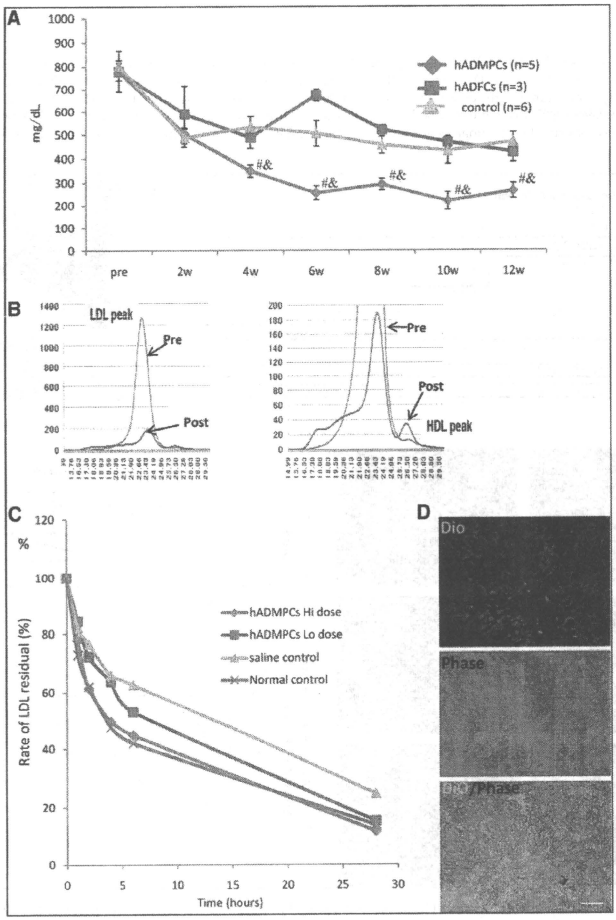

FIG. 3. **(A)** Total serum cholesterol levels. hADMPC transplantation in WHHL rabbits was followed for 12 weeks. Total serum cholesterol was measured in five rabbits that each received 3×10^7 hADMPCs, three rabbits that each received 3×10^7 hADFCs, and in six rabbits that received saline (control). Bars indicated mean ± standard error of the mean (SEM) ($^{\#}p < 0.05$; control vs. the hADMPC-transplanted WHHL rabbit; $^{\&}p < 0.05$; the hADFC-transplanted WHHL rabbit vs. the hADMPC-transplanted WHHL rabbit). **(B)** Lipoprotein profiles in a representative WHHL rabbit with hADMPC transplantation after gel filtration. Serum samples from the WHHL rabbit before and 4 weeks after transplantation were fractionated. Note the marked reduction in low-density lipoprotein (LDL) peak and appearance of high-density lipoprotein (HDL) peak. **(C)** Rate of clearance of LDL from the serum of rabbits with and without transplantation of hADMPCs. Animals were injected with ^{125}I-labeled human LDL, and the time course of clearance was monitored following trichroloacetic acid precipitation of serum at time 5 min, 1 h, 2 h, 4 h, 6 h, and 28 h. Residual ^{125}I-LDL was expressed as percentages of that at 5 min. $^{\#}p < 0.05$ (control vs. the hADMPC-transplanted WHHL rabbit [low dose]) and $^{*}p < 0.05$ (control vs. the hADMPC-transplanted WHHL rabbit [high dose]). **(D)** DiO-LDL uptake into hADMPC-derived hepatocytes in the WHHL rabbi liver. Thin-sliced recipient liver was incubated with DiO-labeled LDL in the serum-free medium for 24 h. After washing and fixation, the incubated slices were applied for fluorescent microscopy. DiO-LDL uptake cells (green) and no uptake parenchymal cells were observed in the section. Bar = 100 μm.

drogenase expression. To confirm that hADMPCs differentiated into hepatocytes *in vivo*, the cells before transplantation and human primary hepatocytes (Invitrogen, Lot number; HuP81) were applied for quantitative PCR as control.

Clearance of ^{125}I-LDL from rabbit serum

WHHL rabbits (8 weeks old) were anesthetized with pentobarbital (50 mg/kg). The peritoneum was incised and hADMPCs (high-dose; 3×10^7 cells/rabbit, $n=2$, low-dose; 5×10^6 cells/rabbit, $n=2$) suspended in 3 mL of HBSS (20°C) ($n=5$) or 3 mL of control saline ($n=2$) were infused into the portal vein via a 18-gauge Angiocath (BD). The rabbits were immunosuppressed using the protocol illustrated in Figure 1A. Eight weeks later, the animals were tested by the LDL turnover assay. ^{125}I human LDL (BT-913R, Lot No. 9130709; Biomedical Technologies Inc.) was delivered via the marginal ear vein of the WHHL rabbits and normal control

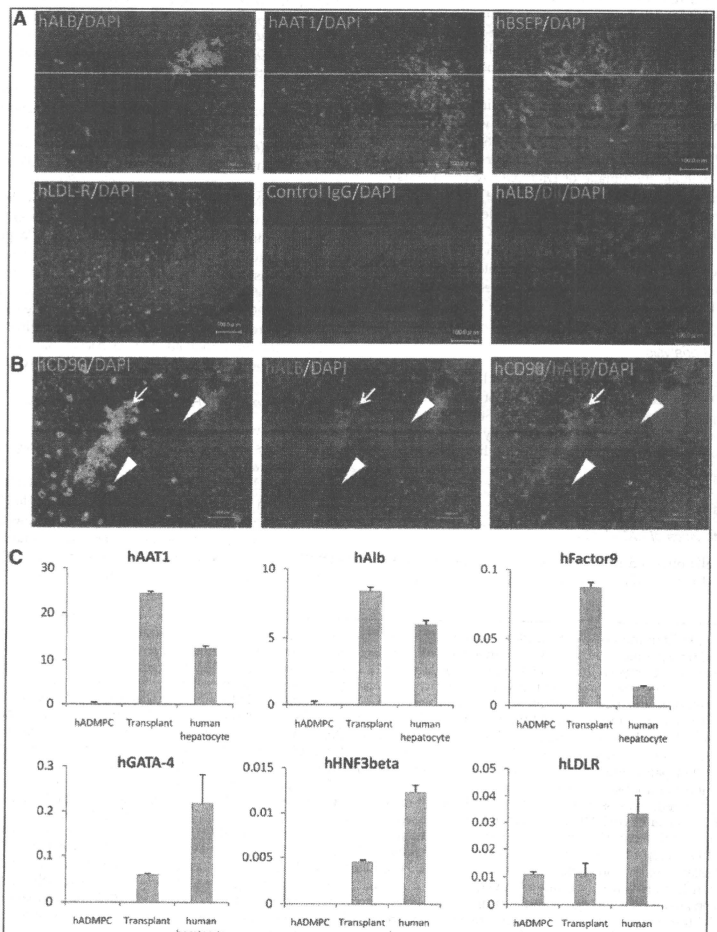

rabbits in physiological saline containing 2 mg/mL bovine serum albumin. Blood was collected from the opposite ear after injection at 5 min, 1 h, 2 h, 4 h, 6 h, and 28 h. ^{125}I-labeled apolipoprotein B-containing LDL was precipitated with 20% of trichloroacetic acid (Wako Pure Chemical Industries) (serum; 320 μL, 100% w/v trichloroacetic acid (TCA) 80 μL), and then the precipitants were applied for counting.

Uptake of DiO-labeled LDL by transplants ex vivo

Human LDL (1.019–1.063 g/mL) was isolated by sequential ultracentrifugation from normolipidemic donors as previously described,[24] dialyzed against saline-EDTA, and then sterilized by filtration through a 0.2 μm filter. Lipoproteins were labeled with 3,3′-dioctadecyloxacarbocyanine perchlorate (DiO; Sigma) by incubating the LDL in 0.5% bovine serum albumin/PBS with 100 mL DiO in dimethyl sulfoxide (3 mg/mL) for 8 h at 37°C. The lipoproteins were obtained by sequential ultra centrifugation (1.019–1.063 g/mL) as described,[14] and then dialyzed against PBS and filtered before use. To evaluate the uptake of DiO-LDL by transplants *ex vivo*, thin-sliced WHHL rabbit liver tissue were incubated with serum-free Dulbecco's modified Eagle's medium containing 10 μg/mL DiO-LDL for 24 h at 37°C. Finally, the incubated slices were rinsed, fixed with 10% formalin, sectioned into 5 μm thickness, and mounted with Perma-Flour (Japan Tanner Corporation). The slides were examined using a BioZero laser scanning microscope (Kyence).

Statistical analysis

Values were expressed as mean ± standard error of the mean. Differences between mean values of treated and untreated groups were evaluated using the Student's *t*-test. A *p*-value < 0.05 was considered statistically significant. All statistical analyses were performed using the SPSS Statistics 17.0 package (SPSS Inc.).

Results

Characteristics of hADMPCs

The cells obtained from adipose tissue were seeded and incubated for 24 h (Fig. 1Ai). After incubation, the adherent cells were treated with EDTA solution, and the resulting suspended cells were replated at a density of 10,000 cells/cm^2 on human fibronectin-coated dishes (BD BioCoat) (Fig. 1Aii and 1Aiii). Within two to three passages after the initial plating of the primary culture, hADMPCs appeared as a monolayer of large flat cells (25–30 μm in diameter). As the cells approached confluence, they assumed a more spindle-shaped, fibroblastic morphology (Fig. 1Aiv). After passaging five to six times, the hADMPCs were applied for transplantation. We used flow cytometry to assess markers expressed by hADMPCs (Fig. 1B). The cells were negative for markers of the hematopoietic lineage (CD45) and of hematopoietic stem cells, ABCG-2, CD34, and CD133. They were also negative for CD31, an endothelial cell-associated marker and the surface antigen c-Kit (CD117). However, they stained positively for a number of surface markers characteristic of mesenchymal and/or neural stem cells, but not embryonic stem cells, including CD29, CD44 (hyaluronan receptor), CD73, CD105 (endoglin), and CD166. hADMPCs also were positive for stage-specific embryonic antigen-4. Next, adipogenic, osteogenic, and chondrogenic differentiation potential of hADMPCs were examined (Fig. 1C). Adipogenic differentiation was induced by culture with differentiation medium containing 1-methyl-3-isobutylxanthine (a peroxisome proliferator-activated receptor γ agonist), dexamethasone, and insulin. Induction was confirmed by the accumulation of intracellular lipid droplets that were stained with Oil Red O. After 7-day induction for osteogenesis, hADMPCs were stained with Alizarin red S for mineralized nodules. hADMPCs showed intense Alcian Blue staining, indicating chondrogenic induction capability of hADMPCs.

Serum cholesterol in WHHL rabbit with transplants

hADMPCs were separated from human subcutaneous adipose tissues, cultured for five to seven passages, and applied for transplantation into WHHL rabbits. WHHL rabbits received immunosuppressants and an antiviral agent as illustrated in Figure 2A, and then were transplanted 3×10^7 hADMPCs by portal vein infusion (Fig. 2B). At the day of and 1, 2, 4, 6, and 10 weeks after transplantation of hADMPCs via the portal vein, we examined whether the cells reside or not in the liver after transplantation. Typical

FIG. 4. **(A)** Immunohistochemical identification of human hepatocytic marker cells in liver sections of WHHL rabbits after hADMPC transplantation. Twelve weeks after hADMPC transplantation, human albumin-, human alpha-1-antitrypsin-, human bile salt export pump (BSEP)-, and LDL-receptor-positive cells were dispersed within the perivenous regions of the liver parenchyma, where they made contact with and integrated among the host cells with cell–cell interactions between hADMPC-derived cells and diseased hepatocytes pair. Ten weeks after transplantation of DiI-stained hADMPCs, copresence of human albumin (green) and pretreated DiI-fluorescence (red) on the same cells was observed. Bar = 100 μm. **(B)** Differentiation of transplanted hADMPCs into hepatocyte-like cells. Twelve weeks after transplantation, almost but not all human CD90-positive cells expressed human albumin, indicating that major population of transplanted hADMPCs could differentiate into hepatocyte-like cells (left panel: human CD90; middle panel: human albumin; right panel: merge). Arrows indicate human CD90 and human albumin double-positive cells; arrowheads indicate human CD90-positive but human albumin-negative cells. **(C)** Human hepatic gene expression in WHHL rabbit liver after hADMPC transplantation. RNA was prepared from the WHHL rabbit liver 12 weeks after hADMPC transplantation. We used the following hepatic markers: human alpha-1-antitrypsin, human albumin, human factor IX, human GATA-binding protein 4 (GATA-4), human hepatocyte nuclear factor 3 (HNF-3) beta, and human LDL-receptor. Their expression levels were examined by quantitative real time-polymerase chain reaction (RT-PCR) using Assays-on-Demand Gene Expression Assay Mix. The livers of WHHL rabbits that received saline ($n = 3$) were negative for human hepatic genes. The mRNA levels were normalized based on human glyceraldehyde-3-phosphate dehydrogenase expression as housekeeping gene and data are mean ± SEM of triplicate experiments. The livers of WHHL rabbits that received hADMPC transplantation ($n = 3$) were positive for human hepatic genes, and their expression levels were similar to those of human primary hepatocytes but not hADMPCs *per se*. Data are mean ± SEM.

distribution patterns of transplanted hADMPCs were followed in Figure 2C. DiI-fluorescent labeled-hADMPCs resided and distributed in the portal area at the day of transplantation. Six and 10 weeks after transplantation, DiI-positive transplanted cells migrated into centrilobular direction. Next, to demonstrate certain percentage of repopulation of the transplanted cells in the liver, the ratios of human-derived cell repopulation were examined by analyzing a repetitive DNA sequence at the day of and 2, 4, 6, and 12 weeks after transplantation (Fig. 2D). To indicate standard curve, we mixed the indicated percentage of hADMPCs with rabbit hepatocytes and plotted the obtained the amount of *Alu* PCR products, and estimated the amount of repopulation of the transplanted cells in the liver. At the day of transplantation, the ratio of hADMPCs to whole WHHL rabbit liver cells was $0.21\% \pm 0.056\%$ (mean ± standard error of the mean) and the ratio decreased to $0.016\% \pm 0.002\%$, $0.011\% \pm 0.001\%$, and $0.009\% \pm 0.0001\%$ after 2, 4, and 8 weeks of transplantation, respectively. After 12 weeks of transplantation, the ratio was increased to $0.024\% \pm 0.00005\%$ as indicated (Fig. 2D).

To reveal the effects of hADMPC transplantation onto the lipid profiles of the WHHL rabbit, serum cholesterol levels were monitored over 12 weeks (Fig. 3A). Significant reductions in total serum cholesterol were observed within 4 weeks of the transplantation, and the reductions were maintained for the entire period. The reduction in serum cholesterol in the animals that received hADMPC transplantation was significantly greater than that of the control group. To determine the effects of hADMPC transplantation on the fractions of high-density lipoprotein and LDL in recipient animals, fractionation by fast protein liquid chromatography was performed (Fig. 3B). Transplantation of hADMPCs resulted in marked reduction of the peak LDL-cholesterol and increment of high-density lipoprotein cholesterol fraction (right panel).

Next, clearance experiments were performed with human LDL to confirm that the transplanted hADMPCs contributed the fall in serum cholesterol through uptake of LDL via LDL receptors. The rate of LDL clearance was significantly higher in the WHHL rabbits with transplanted hADMPCs than WHHL rabbits without transplanted hADMPCs (Fig. 3C). Rabbits with hADMPC transplants showed ~2.4-fold (high-dose; 3×10^7 cells/rabbit) and 1.4-fold (low-dose; 5×10^6 cells/rabbit) increase in the rate of LDL cholesterol clearance.

To evaluate the uptake of DiO-LDL by transplants *ex vivo*, thin-sliced WHHL rabbit liver was incubated with DiO-labeled LDL for 24 h and the uptake was examined as clearance experiment (Fig. 3D). DiO-LDL was uptaken by some but not all of the cells in the WHHL rabbit liver transplanted with hADMPCs. The DiO-LDL-uptaking cells were seen dispersed, contacted, and integrated among the nonuptaking parenchymal cells, suggesting that hADMPCs differentiated into hepatocytes *in vivo*, lowered of serum cholesterol via LDL uptake.

hADMPCs reside, survive, and differentiate into hepatocytes in vivo

After establishment of the graft as indicated by long-term lowering of serum cholesterol, human-specific hepatocytic proteins, such as albumin, alpha-1-antitrypsin, bile salt export pump, and LDL-receptor, positive cells were identified dispersed within perivenous regions of the liver parenchyma, where they have contacted and integrated among the host cells (Fig. 4A), with cell–cell interactions conserved between hADMPC-derived hepatocytes and diseased hepatocytes pair. Ten weeks after transplantation of DiI-prestained hADMPCs, copresence of human albumin (green) and pretreated DiI-fluorescence (red) on the same cells was observed (Fig. 4A), indicating the transplanted hADMPCs might differentiate into hepatocyte-like cells. To confirm transplanted hADMPCs might differentiate into hepatocyte-like cells and to reveal the efficacy of differentiation, the colocalization of human CD90 and human albumin was examined. As shown in Figure 4B, almost but not all human CD90-positive cells expressed human albumin, indicating that about 80% or more of transplanted hADMPCs could differentiated into human albumin-positive hepatocyte-like cells 12 weeks after transplantation. Next, to confirm the differentiation of hADMPCs into hepatocytes *in vivo*, expression of hepatocyte markers was analyzed by quantitative RT-PCR. The WHHL rabbit liver that was transplanted with hADMPCs expressed higher levels of human-specific alpha-1-antitrypsin, albumin, and coagulation factor IX than hADMPCs (Fig. 4C). The expression levels of human GATA-4, human hepatocyte nuclear factor 3 beta, and LDL-receptor were also higher in the WHHL rabbit liver than hADMPCs (Fig. 4C). These results indicate that hADMPCs differentiate into mature hepatocytes *in vivo*.

Discussion

We have used the WHHL rabbit to study the ability of hADMPC-derived hepatocytes to lower serum cholesterol in an animal model of FH. Our results have shown that hADMPCs transplanted into the rabbit liver differentiate into hepatocytes *in vivo* and effectively clear LDL from the circulation.

The reductions in cholesterol brought about by the engrafted hADMPC-derived hepatocytes suggest that human LDL receptors can act as replacement for the mutant LDL receptors in the WHHL rabbit. This capacity of hADMPC-derive hepatocytes is not unexpected, as the liver is the most important site of LDL uptake, accounting for >50% of total removal from the circulation, and the liver is only organ capable of converting cholesterol to bile for excretion. The substantial decrease in serum cholesterol achieved suggests that the hADMPC-derived hepatocytes both internalize LDL and metabolize the cholesterol to bile for excretion. The correlation between cholesterol and coronary heart disease has been well documented, and decreases in serum cholesterol of the magnitude that we have demonstrated would be expected to decrease morbidity and mortality in the patients with severe FH.[25]

The appearance of the hADMPC-derived hepatocytes as revealed by immunohistochemistry and RT-PCR indicated that the hADMPCs differentiated into hepatocytes and integrated into the liver parenchyma. The perivenous migration of the differentiated hepatocytes derived from hADMPCs along the portal-venous axis and suggests that hADMPCs recognize conserved signals on host cells and matrix. There are some reports describing the hepatogenic differentiation potential of hADMPCs.[15,16] These studies

described that hepatocytes differentiated from hADMPCs *ex vivo* engrafted in the liver and functioned, and that the hADMPCs could be resided and changed their characters into hepatocyte-like cells only in the chemically damaged liver. These reports, revealing that hADMPCs have capabilities to differentiate into hepatocytes, hinted us that hADMPCs might differentiate into hepatocytes in liver. Hepatogenic signals from the microenvironment such as cell-to-cell connections or intermediates are probably important factors that dictate the type of functional hepatocytes in hepatic differentiation.[26] We are currently investigating the mechanism for the differentiation hADMPCs into hepatocytes.

The choice of cell source is critical for realizing success in cellular therapy. Liposuction surgeries yield a massive amount of lipoaspirate adipose tissue from 100 mL to >3 L as cell sources.[27] A major advantage of hADMPCs is their availability in safe and easy with few ethical issues, as compared with the shortage of human livers for orthotopic transplantation, which has been shown to be effective for the treatment of FH.[25] Our serum cholesterol reduction studies and *in vitro* studies demonstrated that human LDL binds to the hADMPC-derived hepatocytes receptor, indicating that this therapy will be useful in humans. Previous attempts to study the efficacy of hepatocyte transplantation in the WHHL rabbit model have employed allogenic hepatocytes, xenogenic hepatocytes, or hepatocytes transduced *ex vivo* with a recombinant retrovirus containing the LDL receptor cDNA.[6–13] The lowering effects of hepatocyte transplantation on serum cholesterol have been reported, but there was some problems. First, hepatocytes could not be expanded *ex vivo* with functional potentials; second, the cell viability reduced after cryopreservation; third, the many injected hepatocytes are supposed to be cleared by the reticuloendothelial system or lose viability during early phase. The rate of LDL clearance was returned to normal in LDL receptor knockout mice by introduction of an adenoviral construct containing an LDL receptor cDNA, and similar approaches have lowered serum cholesterol levels in the WHHL rabbit.[10,12,13] However, sustained expression of the LDL receptor from viral vectors can be difficult to achieve.[11,13] Moreover, hepatocytes derived from hADMPCs have the advantage that the LDL receptor is expressed from an endogenous gene with intact regulatory sequences. Such control of LDL receptor levels would not be expected after treatment of hypercholesterolemia with LDL receptor cDNA construct that lack the regulatory regions of the gene.[28]

Our experiments have shown that the hADMPCs expressed hepatocyte markers after transplantation *in vivo* and the integrated cells into parenchyma provide functional LDL receptors, indicating that they differentiated into hepatocytes and might lower serum cholesterol in the WHHL rabbit. These results suggested that hADMPC transplantation via portal vein could correct the metabolic defects of FH patients and that hADMPC-derived hepatocytes could function as supplier with plasma proteins derived from liver, giving us an idea that hADMPC-transplantation might be a novel cell therapy for hemophilia, alpha-1 antitrypsin deficiency, mucolipidosis, and other diseases caused by genetic defects for liver function. In near future, the therapy will be a novel therapy for kinds of inherited liver diseases.

Acknowledgments

This study was supported in part by the Program for Promotion of Fundamental Studies in Health Sciences of the National Institute of Biomedical Innovation (NIBIO), RIKEN Program for Drug Discovery and Medical Technology Platforms, and Kobe Translational Research Cluster, the Knowledge Cluster Initiative, Ministry of Education, Culture, Sports, Science and Technology (MEXT).

Disclosure Statement

All of the authors stated no conflict of interest.

References

1. Brown, M.S., and Goldstein, J.L. A receptor-mediated pathway for cholesterol homeostasis. Science **232,** 34, 1986.
2. Havel, R.J., Yamada, N., and Shames, D.M. Watanabe heritable hyperlipidemic rabbit. Animal model for familial hypercholesterolemia. Arteriosclerosis **9(1 Suppl),** I33, 1989.
3. Yamamoto, T., Bishop, R.W., Brown, M.S., Goldstein, J.L., and Russell, D.W. Deletion in cysteine-rich region of LDL receptor impedes transport to cell surface in WHHL rabbit. Science **32,** 1230, 1986.
4. Bujo, H., Takahashi, K., Saito, Y., Maruyama, T., Yamashita, S., Matsuzawa, Y., Ishibashi, S., Shionoiri, F., Yamada, N., and Kita, T. Clinical features of familial hypercholesterolemia in Japan in a database from 1996–1998 by the research committee of the ministry of health, labour and welfare of Japan. J Atheroscler Thromb **11,** 146, 2004.
5. Yamashita, S., Hbujo, H., Arai, H., Harada-Shiba, M., Matsui, S., Fukushima, M., Saito, Y., Kita, T., and Matsuzawa, Y. Long-term probucol treatment prevents secondary cardiovascular events: a cohort study of patients with heterozygous familial hypercholesterolemia in Japan. J Atheroscler Thromb **15,** 292, 2008.
6. Gunsalus, J.R., Brady, D.A., Coulter, S.M., Gray, B.M., and Edge, A.S. Reduction of serum cholesterol in Watanabe rabbits by xenogeneic hepatocellular transplantation. Nat Med **3,** 48, 1997.
7. Tejera, M.L., Cienfuegos, J.A., Maganto, P., Pardo, F., Santamaria, L., Codesal, J., De Andres, S., Hernandez, J.L., and Castillo-Olivares, J.L. Reduction of cholesterol levels following liver cell grafting in hyperlipidemic (WHHL) rabbits. Transplant Proc **24,** 160, 1992.
8. Wang, J., Pollak, R., and Bartholomew, A. Sustained reduction of serum cholesterol levels following allo-transplantation of parenchymal hepatocytes in Watanabe rabbits. Transplant Proc **23,** 894, 1991.
9. Wiederkehr, J.C., Kondos, G.T., and Pollak, R. Hepatocyte transplantation for the low-density lipoprotein receptor-deficient state. A study in the Watanabe rabbit. Transplantation **50,** 466, 1990.
10. Chowdhury, J.R., Grossman, M., Gupta, S., Chowdhury, N.R., Baker, J.R., Jr., and Wilson, J.M. Long-term improvement of hypercholesterolemia after *ex vivo* gene therapy in LDLR-deficient rabbits. Science **254,** 1802, 1991.
11. Ishibashi, S., Brown, M.S., Goldstein, J.L., Gerard, R.D., Hammer, R.E., and Herz, J. Hypercholesterolemia in low density lipoprotein receptor knockout mice and its reversal by adenovirus-mediated gene delivery. J Clin Invest **92,** 883, 1993.
12. Kozarsky, K.F., McKinley, D.R., Austin, L.L., Raper, S.E., Stratford-Perricaudet, L.D., and Wilson, J.M. *In vivo* correction

of low density lipoprotein receptor deficiency in the Watanabe heritable hyperlipidemic rabbit with recombinant adenoviruses. J Biol Chem **269,** 13695, 1994.
13. Wilson, J.M., Chowdhury, N.R., Grossman, M., Wajsman, R., Epstein, A., Mulligan, R.C., and Chowdhury, J.R. Temporary amelioration of hyperlipidemia in low density lipoprotein receptor-deficient rabbits transplanted with genetically modified hepatocytes. Proc Natl Acad Sci U S A **87,** 8437, 1990.
14. Okura, H., Komoda, H., Saga, A., Kakuta-Yamamoto, A., Hamada, Y., Fumimoto, Y., Lee, C.M., Ichinose, A., Sawa, Y., and Matsuyama, A. Properties of hepatocyte-like cell clusters from human adipose tissue-derived mesenchymal stem cells. Tissue Eng Part C Methods **16,** 761, 2010.
15. Banas, A., Teratani, T., Yamamoto, Y., Tokuhara, M., Takeshita, F., Quinn, G., Okochi, H., and Ochiya, T. Adipose tissue-derived mesenchymal stem cells as a source of human hepatocytes. Hepatology **46,** 219, 2007.
16. Seo, M.J., Suh, S.Y., Bae, Y.C., and Jung, J.S. Differentiation of human adipose stromal cells into hepatic lineage *in vitro* and *in vivo*. Biochem Biophys Res Commun **328,** 258, 2005.
17. Komoda, H., Okura, H., Lee, C.M., Sougawa, N., Iwayama, T., Hashikawa, T., Saga, A., Yamamoto, A., Ichinose, A., Murakami, S., Sawa, Y., and Matsuyama, A. Reduction of N-glycolylneuraminic acid xenoantigen on human adipose tissue-derived stromal cells/mesenchymal stem cells leads to safer and more useful cell sources for various stem cell therapies. Tissue Eng Part A **16,** 1143, 2010.
18. Okura, H., Matsuyama, A., Lee, C.M., Saga, A., Kakuta-Yamamoto, A., Nagao, A., Sougawa, N., Sekiya, N., Takekita, K., Shudo, Y., Miyagawa, S., Komoda, H., Okano, T., and Sawa, Y. Cardiomyoblast-like cells differentiated from human adipose tissue-derived mesenchymal stem cells improve left ventricular dysfunction and survival in a rat myocardial infarction model. Tissue Eng Part C Methods **16,** 417, 2010.
19. Bjorntorp, P., Karlsson, M., Pertoft, H., Pettersson, P., Sjostrom, L., and Smith, U. Isolation and characterization of cells from rat adipose tissue developing into adipocytes. J Lipid Res **19,** 316, 1978.
20. Zuk, P.A., Zhu, M., Ashjian, P., De Ugarte, D.A., Huang, J.I., Mizuno, H., Alfonso, Z.C., Fraser, J.K., Benhaim, P., and Hedrick, M.H. Human adipose tissue is a source of multipotent stem cells. Mol Biol Cell **13,** 4279, 2002.
21. Nicklas, J.A., and Buel, E. Development of an Alu-based, real-time PCR method for quantitation of human DNA in forensic samples. J Forensic Sci **48,** 936, 2003.
22. Opel, K.L., Fleishaker, E.L., Nicklas, J.A., Buel, E., and McCord, B.R. Evaluation and quantification of nuclear DNA from human telogen hairs. J Forensic Sci **53,** 853, 2008.
23. Okazaki, M., Usui, S., Ishigami, M., Sakai, N., Nakamura, T., Matsuzawa, Y., and Yamashita, S. Identification of unique lipoprotein subclasses for visceral obesity by component analysis of cholesterol profile in high-performance liquid chromatography. Arterioscler Thromb Vasc Biol **25,** 578, 2005.
24. Bier, D.M., and Havel, R.J. Activation of lipoprotein lipase by lipoprotein fractions of human serum. J Lipid Res **11,** 565, 1970.
25. Steinberg, D., and Witztum, J.L. Current concepts. Lipoproteins and atherogenesis. Current concepts. JAMA **264,** 3047, 1990.
26. Hughes, R.D., Mitry, R.R., and Dhawan, A. Hepatocyte transplantation for metabolic liver disease: UK experience. J R Soc Med **98,** 341, 2005.
27. Gimble, J.M., Katz, A.J., and Bunnell, B.A. Adipose-derived stem cells for regenerative medicine. Circ Res **100,** 1249, 2007.
28. Bilheimer, D.W., Goldstein, J.L., Grundy, S.M., Starzl, T.E., and Brown, M.S. Liver transplantation to provide low-density-lipoprotein receptors and lower plasma cholesterol in a child with homozygous familial hypercholesterolemia. N Engl J Med **311,** 1658, 1984.

Address correspondence to:
Akifumi Matsuyama, M.D., Ph.D.
Department of Somatic Stem Cell Therapy and Health Policy
Foundation for Biomedical Research and Innovation
TRI305, 1-5-4 Minatojima-minamimachi, Chuo-ku
Kobe 650-0047
Japan

E-mail: akifumi-matsuyama@umin.ac.jp

Received: March 7, 2010
Accepted: August 9, 2010
Online Publication Date: September 21, 2010

Fujii et al. Radiation Oncology 2011, 6:8
http://www.ro-journal.com/content/6/1/8

RADIATION ONCOLOGY

RESEARCH Open Access

Cationized gelatin-HVJ envelope with sodium borocaptate improved the BNCT efficacy for liver tumors *in vivo*

Hitoshi Fujii[1], Akifumi Matsuyama[2], Hiroshi Komoda[1], Masao Sasai[2], Minoru Suzuki[3], Tomoyuki Asano[4], Yuichiro Doki[1], Mitsunori Kirihata[4], Koji Ono[3], Yasuhiko Tabata[5], Yasufumi Kaneda[6], Yoshiki Sawa[1], Chun Man Lee[1,2,7*]

Abstract

Background: Boron neutron capture therapy (BNCT) is a cell-selective radiation therapy that uses the alpha particles and lithium nuclei produced by the boron neutron capture reaction. BNCT is a relatively safe tool for treating multiple or diffuse malignant tumors with little injury to normal tissue. The success or failure of BNCT depends upon the ^{10}B compound accumulation within tumor cells and the proximity of the tumor cells to the body surface. To extend the therapeutic use of BNCT from surface tumors to visceral tumors will require ^{10}B compounds that accumulate strongly in tumor cells without significant accumulation in normal cells, and an appropriate delivery method for deeper tissues.
Hemagglutinating Virus of Japan Envelope (HVJ-E) is used as a vehicle for gene delivery because of its high ability to fuse with cells. However, its strong hemagglutination activity makes HVJ-E unsuitable for systemic administration. In this study, we developed a novel vector for ^{10}B (sodium borocaptate: BSH) delivery using HVJ-E and cationized gelatin for treating multiple liver tumors with BNCT without severe adverse events.

Methods: We developed cationized gelatin conjugate HVJ-E combined with BSH (CG-HVJ-E-BSH), and evaluated its characteristics (toxicity, affinity for tumor cells, accumulation and retention in tumor cells, boron-carrying capacity to multiple liver tumors *in vivo*, and bio-distribution) and effectiveness in BNCT therapy in a murine model of multiple liver tumors.

Results: CG-HVJ-E reduced hemagglutination activity by half and was significantly less toxic in mice than HVJ-E. Higher ^{10}B concentrations in murine osteosarcoma cells (LM8G5) were achieved with CG-HVJ-E-BSH than with BSH. When administered into mice bearing multiple LM8G5 liver tumors, the tumor/normal liver ratios of CG-HVJ-E-BSH were significantly higher than those of BSH for the first 48 hours ($p < 0.05$). In suppressing the spread of tumor cells in mice, BNCT treatment was as effective with CG-HVJ-E-BSH as with BSH containing a 35-fold higher ^{10}B dose. Furthermore, CG-HVJ-E-BSH significantly increased the survival time of tumor-bearing mice compared to BSH at a comparable dosage of ^{10}B.

Conclusion: CG-HVJ-E-BSH is a promising strategy for the BNCT treatment of visceral tumors without severe adverse events to surrounding normal tissues.

* Correspondence: tg4c_1211@help.med.osaka-u.ac.jp
[1]Department of Surgery, Osaka University Graduate School of Medicine, Osaka, Japan
Full list of author information is available at the end of the article

Background

Boron neutron capture therapy (BNCT) is a cell-selective radiation therapy that uses alpha particles and lithium nuclei produced by the boron neutron capture reaction. These particles cause cell destruction, bouncing out to a maximum distance of 10 μm from the target, a distance that corresponds to the size of a cell. These particles only destroy the cells that take up ^{10}Boron (^{10}B) [1]. This therapy is clinically indicated for multiple and diffuse tumors, such as glioblastoma and head and neck tumors [2]. BNCT was recently evaluated for treating liver tumors [3-8], although the prognosis of patients treated by BNCT with conventional ^{10}B compounds, particularly sodium borocaptate (BSH), is not good because of its low accumulation in liver tumors and the attenuation of the epithermal neutron beams directed toward deep lesions [9-11]. Therefore, treating liver tumors effectively with BNCT will require novel ways of delivering BSH, with the characteristics of high accumulation in the tumor, low toxicity for normal tissue, and rapid withdrawal from normal tissue and the bloodstream [12]. Various carriers such as liposomes have been investigated [13-16], but until now a vector for BSH that adequately satisfies the above requirements has not been developed.

Liver tumors, including primary and secondary tumors, are the fifth most common solid tumor worldwide. The incidence is increasing rapidly in most countries, at a pace that will make liver tumors the third most common tumor by 2030 [17,18]. The mortality rate of liver tumors, especially multiple metastatic liver tumors, is high. Multimodal therapies for multiple liver tumors have advanced considerably, and include radiofrequency ablation, radiation, surgical extirpation and transplantation [19]. However, therapy for multiple and diffuse liver tumors is still difficult, because reducing the liver volume reduces its organ function. Therefore, a therapy selective for tumors with minimal damage to normal liver tissue is of great interest.

Hemagglutinating Virus of Japan Envelope (HVJ-E) is a simple vector that is converted into an inactivated virus containing lipid envelope for gene transfer vector originally [20]. HVJ-E has been used to carry anticancer drugs with some success [21,22]. HVJ-E is reported both to possess high fusion ability and to elicit anti-tumor immune responses [23,24], making it an attractive candidate for widespread use in cancer therapy. On the other hand, HVJ-E has strong hemagglutination activity, making it unsuitable to administer systemically. There are no reports describing the systemic administration of HVJ-E in cancer therapy, although one study reports improved HVJ-E stability in the bloodstream when it is administered with a cationized gelatin [25]. The development of a novel HVJ-E-based vector that can be administered into the general circulation is highly desirable for cancer treatment.

We therefore focused on HVJ-E because of its versatility, its high fusion ability, and its ability to stimulate an immune response. We developed a cationized gelatin conjugate of HVJ-E with BSH that can be administered into the general circulation, and we evaluated its safety, bio-distribution, and effectiveness in BNCT treatment using a murine model of multiple liver tumors.

Materials and methods

Mice

Female C3H/HeN Jcl mice at 8-12 weeks of age were obtained from CLEA Japan (Tokyo, Japan) and kept in standard housing. Body weight of mice was 19.6 ± 1.6 (17-23) g at each experiment. All animal experiments were performed under a protocol approved by the Ethics Review Committee for Animal Experimentation of Osaka University Graduate School of Medicine.

Cell line

The cell line of murine osteosarcoma (LM8G5), which was isolated from LM8 cells after five successive cycles of *in vivo* selection procedures, were used because of their high potential for metastasizing to the liver [26,27]. The cells were maintained in D-MEM (Sigma Aldrich Japan, Tokyo, Japan) containing 10% fetal bovine serum, 1% (v/v) 100 × non-essential amino acids, 1 mM sodium pyruvate, 2 mM L-glutamine, 50 μM 2-mercaptoethanol, 100 units/ml penicillin, and 100 μg/ml streptomycin.

Animal Model

LM8G5 cells (1×10^6 cells in 200 μl, with serum-free medium) were injected into the surgically exposed ileocolic vein of mice under general anesthesia with Avertin (2.5% tribromoethanol at a concentration of 1 ml/100 g live weight). Multiple small liver tumors were observed seven days after the injection by exploratory laparotomy, and these tumors led to the death of the mice within 20 days after tumor inoculation.

HVJ-E

HVJ was purified from chicken egg chorioallantoic fluid by centrifugation, and the titer calculated as previously described [20]. The virus was inactivated by UV irradiation exposure (99 mJ/cm^2) just before use, eliminating the ability of the virus to replicate while leaving its fusion capacity intact, as previously described [20].

Cationized Gelatin (CG) and BSH

Gelatin was prepared from pig skin type I collagen through an acid process, and was kindly supplied by Nitta Gelatin (Osaka, Japan). Ethylenediamine (ED),